

## Detecting event-related time-dependent directional couplings

R G Andrzejak<sup>1</sup>, A Ledberg<sup>1</sup> and G Deco<sup>1,2</sup>

<sup>1</sup> Universitat Pompeu Fabra, Department of Technology,  
Passeig de Circumval·lació 8, 08003 Barcelona, Spain

<sup>2</sup> Institució Catalana de Recerca i Estudis Avançats (ICREA), Passeig Lluís  
Comanys 23, 08010 Barcelona, Spain

E-mail: [ralph.andrzejak@upf.edu](mailto:ralph.andrzejak@upf.edu)

*New Journal of Physics* **8** (2006) 6

Received 18 October 2005

Published 25 January 2006

Online at <http://www.njp.org/>

doi:10.1088/1367-2630/8/1/006

**Abstract.** Nonlinear interdependence measures can be used to detect directional couplings between stationary dynamical systems from a pair of signals measured from them. For many dynamics, however, intermittent directional couplings arise in causal relation to distinct events on timescales that are often too short to be resolved by nonlinear interdependence measures. On the other hand, in many experimental settings signals are measured for multiple instances of such events. We demonstrate how these multiple realizations can be exploited to reliably detect event-related time-dependent directional couplings. For this purpose, we propose the general concept of time-resolved causal statistics derived from embeddings across multiple realizations of time-dependent dynamics. Surrogates constructed by permuting the order of realizations can be used to test specified null hypotheses. We adapt a conventional nonlinear interdependence measure to serve as a time-resolved causal statistic and apply it to exemplary coupled Lorenz dynamics. This approach allows detecting event-related time-dependent directional couplings based on only a few tens of realizations. Changes of the coupling direction can be detected within one oscillation of the dynamics. Beyond this particular application, any metric bivariate or univariate measure can be adapted to serve as time-resolved causal statistics to characterize various aspects of event-related time-dependent dynamics.

A detection of directional couplings between two distinct dynamical systems  $X$  and  $Y$  from the analysis of pairs of signals measured from them is key to an understanding of many dynamics in nature. To detect directional couplings phase dynamics estimates [1] as well as estimates based

on the reconstruction of state spaces (e.g. [2]–[4]) have been proposed. Recent applications can be found in many different scientific disciplines [5]–[10] and moving window techniques are commonly used to track time-dependent couplings. In particular, in [4] the moving window is implemented already in the coupling detection statistics. For a wide variety of dynamics in nature, however, it can be conjectured that short intermittent couplings arise in causal relation to certain events and that the timescales of these processes are too short to be resolved by moving window techniques. On the other hand, in many experimental settings signals are measured for multiple instances of such events. Therefore, multiple realizations of the corresponding transient dynamics are available. For example, in neuroscience the collection of multivariate signals obtained time-locked to repeated presentations of identical stimuli is very common. Apart from such external events imposed on the system, events related to coupling changes can be inherent to the system, for example epileptic spikes or seismic events, and coupling changes might either be the cause or the consequence of these events. For such internal events, multiple realizations can readily be obtained retrospectively by aligning segments of continuous recordings with regard to the events. In this paper, we show how multiple realizations can be exploited to reliably detect event-related time-dependent directional couplings.

Consider first a single pair of time series  $\{x_i\}$  and  $\{y_i\}$  measured from  $X$  and  $Y$  at discrete times  $i = 0, \dots, n$ . To determine whether  $X$  and  $Y$  are coupled, at first delay vectors [11] can be used to reconstruct the dynamics:  $\mathbf{x}_i = (x_i, \dots, x_{i-(m-1)\tau})$ ,  $\mathbf{y}_i = (y_i, \dots, y_{i-(m-1)\tau})$ . Here,  $m$  and  $\tau$  denote the embedding dimension and delay time, respectively, for  $i = \eta, \dots, n$  with embedding window  $\eta = (m - 1)\tau$ . Subsequently, some nonlinear interdependence measure [2]–[4] can be used to detect a directional coupling between  $X$  and  $Y$  from  $\{\mathbf{x}_i, \mathbf{y}_i\}_{i=\eta, \dots, n}$ . A metric measure was proposed in [3]: the averaged squared distance of  $\mathbf{x}_i$  to all other points in  $\{\mathbf{x}_i\}_{i=\eta, \dots, n}$  is  $R_i(X) = \frac{1}{n-\eta} \sum_{s=\eta, s \neq i}^n |\mathbf{x}_i - \mathbf{x}_s|^2$ . Denoting the time indices of the  $g$  nearest neighbours of  $\mathbf{y}_i$  among  $\{\mathbf{y}_i\}_{i=\eta, \dots, n}$  by  $\{r_{i,l}\}_{l=1, \dots, g}$ , the  $Y$ -conditioned mean-squared Euclidean distance for each  $\mathbf{x}_i$  is defined by  $R_i(X|Y) = \frac{1}{g} \sum_{l=1}^g |\mathbf{x}_i - \mathbf{x}_{r_{i,l}}|^2$ . Finally, one defines:

$$H(X|Y) = \frac{1}{n - \eta + 1} \sum_{i=\eta}^n \log \frac{R_i(X)}{R_i(X|Y)}. \quad (1)$$

The quantity  $H(Y|X)$  is defined by reversing the roles of  $X$  and  $Y$ . In the limit of an infinite number of data points and nearest neighbours the following relations hold: if  $X$  and  $Y$  are independent then both  $H(X|Y)$  and  $H(Y|X)$  go to zero. If there is a coupling from  $X$  to  $Y$  we get  $H(X|Y) > H(Y|X) > 0$ , and analogously  $H(Y|X) > H(X|Y) > 0$  for the other coupling direction. Hence, the coupling direction can be read from the difference of  $H(X|Y)$  and  $H(Y|X)$ . For a more thorough discussion see [3, 12, 13]. However, note that for finite samples certain offsets can occur as we will discuss below in more detail. Furthermore, these relations hold only for moderately weak couplings resulting in unsynchronized motion. For strong couplings inducing synchronous motion the information of directionality cannot be properly derived [1, 3]. The calculation of  $H$ , by which we denote the pair  $H(X|Y)$  and  $H(Y|X)$ , from  $\{\mathbf{x}_i, \mathbf{y}_i\}_{i=\eta, \dots, n}$  assumes  $X$  and  $Y$  to be stationary. Time-dependent couplings  $\varepsilon(t)$  cannot be resolved because  $H$  is obtained from a temporal average.

Consider now an ensemble of pairs of time series  $\{x_i^j\}$  and  $\{y_i^j\}$  ( $i = 0, \dots, n$ ) for  $k$  realizations of an experiment ( $j = 1, \dots, k$ ). Here,  $i$  does not measure absolute time, but the time elapsed since the start of the respective experiment. Furthermore assume that each experiment starts with independent initial conditions  $(x_0^j, y_0^j)$  and that the time-dependence of

the coupling between  $X$  and  $Y$  is the same for all realizations,  $\varepsilon^1(t) = \dots = \varepsilon^k(t)$ . Now construct  $(n - \eta + 1)k$  conventional pairs of delay vectors  $\{\mathbf{x}_i^j, \mathbf{y}_i^j\}_{i=\eta, \dots, n}^{j=1, \dots, k}$ . For each  $i$ , form embeddings across realizations by grouping  $k$  pairs of delay vectors  $\{\mathbf{x}_i^j, \mathbf{y}_i^j\}_{j=1, \dots, k}$ . In this way we get separate embeddings for each time point, and statistics can be calculated in a causal way from a sequence of such embeddings. In the particular case of  $H$ , realization indices take the role of time indices and correspondingly time averages become ensemble averages: for each  $\mathbf{x}_i^j$  determine  $R_i^j(X|Y) = \frac{1}{g} \sum_{l=1}^g |\mathbf{x}_i^j - \mathbf{x}_i^{r_i^{j,l}}|^2$ , where  $r_i^{j,l}$  denotes the realization index of the  $l$ th nearest neighbour of  $\mathbf{y}_i^j$  among  $\{\mathbf{y}_i^j\}_{j=1, \dots, k}$ . Further, define  $R_i^j(X) = \frac{1}{k-1} \sum_{s=1, s \neq j}^k |\mathbf{x}_i^j - \mathbf{x}_i^s|^2$ ,

$$H_i(X|Y) = \frac{1}{k} \sum_{j=1}^k \log \frac{R_i^j(X)}{R_i^j(X|Y)}, \quad (2)$$

and  $H_i(Y|X)$  analogously.<sup>3</sup> Everything stated in the paragraph subsequent to Equation (1) directly transfers to  $H_i$ . But  $H_i$  is a function of time and can be used to estimate time-dependent couplings. In particular, it relies only on the most recent past namely on information from the preceding embedding window  $\eta$ . Note that the number of realizations in an embedding across realizations cannot be directly compared to the number of time points in an embedding across time. To construct  $k$  delay vectors across realizations,  $k \times m$  scalar samples of the time series are used. All  $k$  delay vectors are mutually independent, no sample is used twice. Hence, there is no need to exclude temporally correlated points from the nearest neighbours [14]. In contrast, in conventional embeddings across time  $n^*$  delay vectors are based on only  $n = n^* + \eta - 1$  scalar samples of the time series, except for samples at the time series' ends, each individual scalar sample is used  $m$  times.

As we shall see below, nonzero values of  $H$  (and of  $H_i$ ) can be obtained also for uncoupled dynamics. Furthermore, changes of  $H_i$  versus time might not be specific for time-dependent couplings but might likewise indicate a time-dependence of  $X$  and  $Y$  themselves. Such potential biases are no peculiarity of  $H_i$  but represent a pitfall of many nonlinear measures [15], which has been successfully addressed by the concept of surrogates [16]. In our setting, a surrogate of  $\{\mathbf{x}_i^j, \mathbf{y}_i^j\}$  can be generated by permuting the indices  $j$  of  $Y$ , keeping those of  $X$  fixed. Through this shuffling, the realization-wise pairings of the time series are destroyed whereas the time series themselves are maintained. Applying the statistics  $H_i$  to both the original and a set of such surrogates, each generated using a different random permutation, allows testing the null hypotheses that  $X$  and  $Y$  are arbitrary but independent processes. As described below, we here use these surrogates not primarily to test this null hypotheses but rather for an offset correction. To test further null hypothesis, e.g. 'changes of  $H_i$  versus time are sufficiently explained by time-dependent linear correlations between  $X$  and  $Y$ ', standard bivariate surrogates can be used [16, 17].

We illustrate our approach on coupled Lorenz dynamics [18, 19]. A 4th order Runge–Kutta routine with step size 0.005 and sampling interval  $\Delta t = 0.03$  was used to integrate the dynamics of  $X$  and  $Y$ :

$$X \begin{cases} \dot{u} = 10(v - u) + \vartheta(a - u), \\ \dot{v} = 35u - v - uw, \\ \dot{w} = uv - \frac{8}{3}w, \end{cases} \quad (3)$$

<sup>3</sup> The code for the calculation for  $H_i$  is enclosed as Supplementary material.

$$Y \begin{cases} \dot{a} = 10(b - a) + \alpha(u - a), \\ \dot{b} = 39a - b - ac, \\ \dot{c} = ab - \frac{8}{3}c. \end{cases} \quad (4)$$

For  $j = 1, \dots, k$  realizations the dynamics were integrated starting from  $k$  different random initial conditions. A number of  $10^6$  pre-iterations with  $\vartheta = \alpha = 0$  were performed to ensure that at  $i = 0$  the  $k$  different trials were distributed according to the natural invariant measure of the uncoupled Lorenz dynamics. Subsequently, for each realization,  $i = 0, \dots, 799$  steps were integrated using the time-dependent coupling scheme:  $\vartheta = \alpha = 0$  for  $i \in \mathcal{A} = [0, \dots, 199]$ ;  $\vartheta = 0, \alpha = \varepsilon$  for both  $i \in \mathcal{B} = [200, \dots, 399]$  and  $i \in \mathcal{D} = [500, \dots, 799]$ ; and  $\vartheta = \varepsilon, \alpha = 0$  for  $i \in \mathcal{C} = [400, \dots, 499]$ . The corresponding 800 samples of  $u$  and  $a$  were used as time series  $\{x_i^j\}$  and  $\{y_i^j\}$ , respectively (figure 1(a)). If not stated otherwise we used  $\varepsilon = 4$  and  $k = 100$ . Results are shown for  $m = 10$ ,  $\tau = 2$  and  $g = 1$ . This represents a reasonable parameter setting with regard to common guidelines [15] and the problem at hand. Similar results are obtained for adjacent parameter settings, and we deliberately refrained from any in-sample fine-tuning with regard to results presented below.

Results for the original dynamics,  $H_i$ , and the range obtained for 39 surrogates,  $\{\hat{H}_{i,q}\}_{q=1,\dots,39}$ , are shown in figures 1(b) and (d). First of all, note that consistently  $H_i > 0$  also for the uncoupled dynamics during  $\mathcal{A}$ . This offset from zero is due to a bias in  $H$  when calculated using only very few nearest neighbours<sup>4</sup>, and, correspondingly, this offset is found also in the surrogates. Except for short intermittent excursions,  $H_i(X|Y)$  and  $H_i(Y|X)$  are within their respective surrogate distribution. Hence, for the vast majority of samples in  $\mathcal{A}$ , the surrogates successfully ruled out that nonzero  $H_i$  values indicate a coupling between  $X$  and  $Y$ . The number of remaining false positive null hypotheses rejections can be reduced using a higher number of surrogates. For the other intervals, we find sustained deviations of  $H_i(X|Y)$  and  $H_i(Y|X)$  from the surrogates, and hence the null hypotheses of  $X$  and  $Y$  being independent is correctly rejected for most samples in  $\mathcal{B}$ ,  $\mathcal{C}$  and  $\mathcal{D}$ . A determination of the significance of a certain number of rejections for subsequent samples is nontrivial as they are obtained from subsequent values of the Lorenz dynamics. Hence, these values are correlated, and the tests are dependent. However, it is not the aim of this paper to address this issue, but rather we here use the surrogates to perform the offset correction  $\tilde{H}_i = H_i - \max\{\hat{H}_{i,q}\}$ . Negative values of  $\tilde{H}_i$  are set to zero. The resulting curves  $\tilde{H}_i(X|Y)$  and  $\tilde{H}_i(Y|X)$  are shown in figures 1(c) and (e). During  $\mathcal{B}$  there is coupling from  $X$  to  $Y$ . According to the considerations subsequent to Equation (1), this should result in  $\Delta\tilde{H}_i = \tilde{H}_i(X|Y) - \tilde{H}_i(Y|X) > 0$ . Indeed  $\Delta\tilde{H}_i$  attains positive values shortly after the coupling onset and stays positive until shortly after the onset of the opposite coupling direction at the beginning of  $\mathcal{C}$  (figure 1(f)). Hence, the coupling from  $X$  to  $Y$  during  $\mathcal{B}$  can be determined

<sup>4</sup> To understand this bias, consider some symmetric distribution with mean  $\mu$  from which independent random samples are drawn. For each sample with value  $\lambda$  calculate  $\gamma = \log(\mu/\lambda)$ , and take the average  $\bar{\gamma}$  of  $\gamma$  over all samples. Now perform a notional pairing of the samples such that for each  $\lambda = \mu + \delta$  a corresponding  $\lambda' = \mu - \delta$  is chosen. With a large number of samples this pairing can always be done, at least approximately. Then  $\gamma + \gamma' > 0$ , and hence  $\bar{\gamma}$  has a positive offset. Another offset occurs for asymmetric distributions. Both offsets diminish if at first  $g$  individual samples are drawn, and their average is used for  $\lambda$ , since this average will always tend to  $\mu$  for increasing  $g$ . These considerations transfer to the calculation of  $H_i$  from independent dynamics using only very few versus many nearest neighbours  $g$ . As we here calculate  $H_i$  with  $g = 1$ , we get a very strong bias.

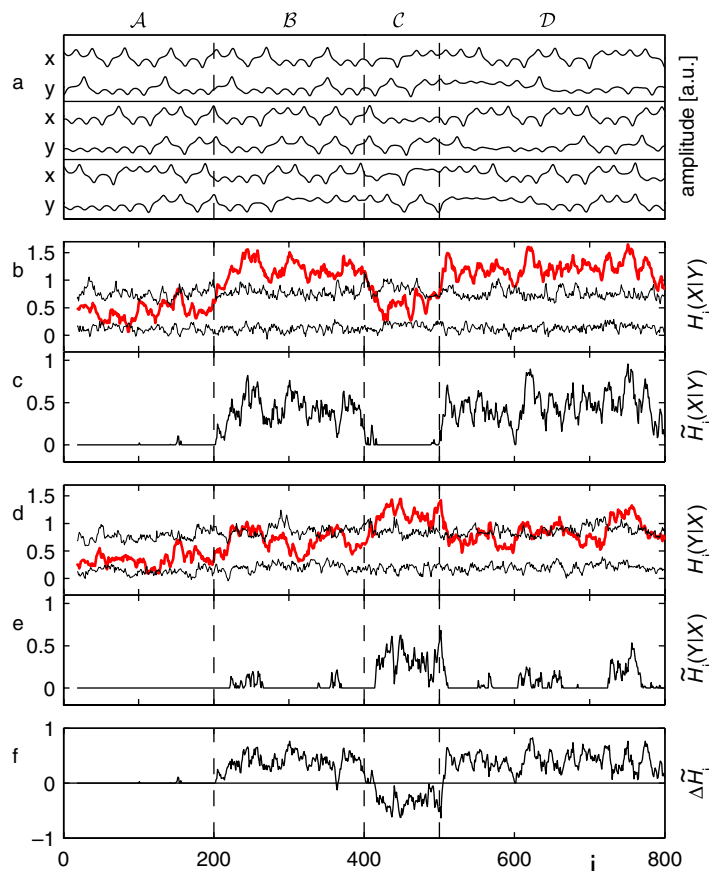


**Figure 1.** (a) Time series for three exemplary realizations. (b and d) Results for the original dynamics (thick red lines) and the range for 39 surrogates (thin black lines). (c and e) Offset corrected results. (f) The difference between the latter. In all panels, vertical lines correspond to the limits between  $\mathcal{A}$  and  $\mathcal{D}$ .

correctly from  $\Delta \tilde{H}_i$ . Furthermore, negative  $\Delta \tilde{H}_i$  values during  $\mathcal{C}$ , and again positive  $\Delta \tilde{H}_i$  values during  $\mathcal{D}$ , correctly indicate the respective coupling direction present in these intervals, again very shortly after the coupling onset.

To study the influence of different parameters, we define the following ad hoc performance measures. At first, we determine the sample index  $i_0$  at which the correct result  $\Delta \tilde{H}_{i_0} > 0$  is found for the first time in  $\mathcal{B}$ . The difference between the beginning of  $\mathcal{B}$  and  $i_0$  is denoted by  $\delta_B$ . The fractions of samples in  $\mathcal{B}$  for which the correct ( $\Delta \tilde{H}_i > 0$ ) and wrong ( $\Delta \tilde{H}_i < 0$ ) result is found between  $i_0$  and the end of  $\mathcal{B}$  are denoted by  $\psi_B$  and  $\psi_B^*$ , respectively. If both  $H_i(X|Y)$  and  $H_i(Y|X)$  are within the respective surrogate range,  $\tilde{H}_i(X|Y) = \tilde{H}_i(Y|X) = 0$ ;  $\Delta \tilde{H}_i = 0$ , and the corresponding sample will neither contribute to  $\psi_B$  nor to  $\psi_B^*$ , hence  $\psi_B + \psi_B^* \leq 1$ . The quantities  $\delta_{C,D}$ ,  $\psi_{C,D}$ , and  $\psi_{C,D}^*$ , are calculated in analogy, taking the opposite coupling direction during  $\mathcal{C}$  into account. We drop the subscripts when we refer to the entire set of measures.

Before we look at the dependence of  $\delta$  and  $\psi$  on the number of realizations, coupling strength, and noise level (figure 2), we shall recall that the dynamics are asymmetric with regard to  $X$  and  $Y$ . Hence, the impact of a coupling from  $X$  to  $Y$  with  $\alpha = \varepsilon$  will not be the same as the impact of a coupling from  $Y$  to  $X$  with the same coupling strength  $\vartheta = \varepsilon$ . Furthermore,

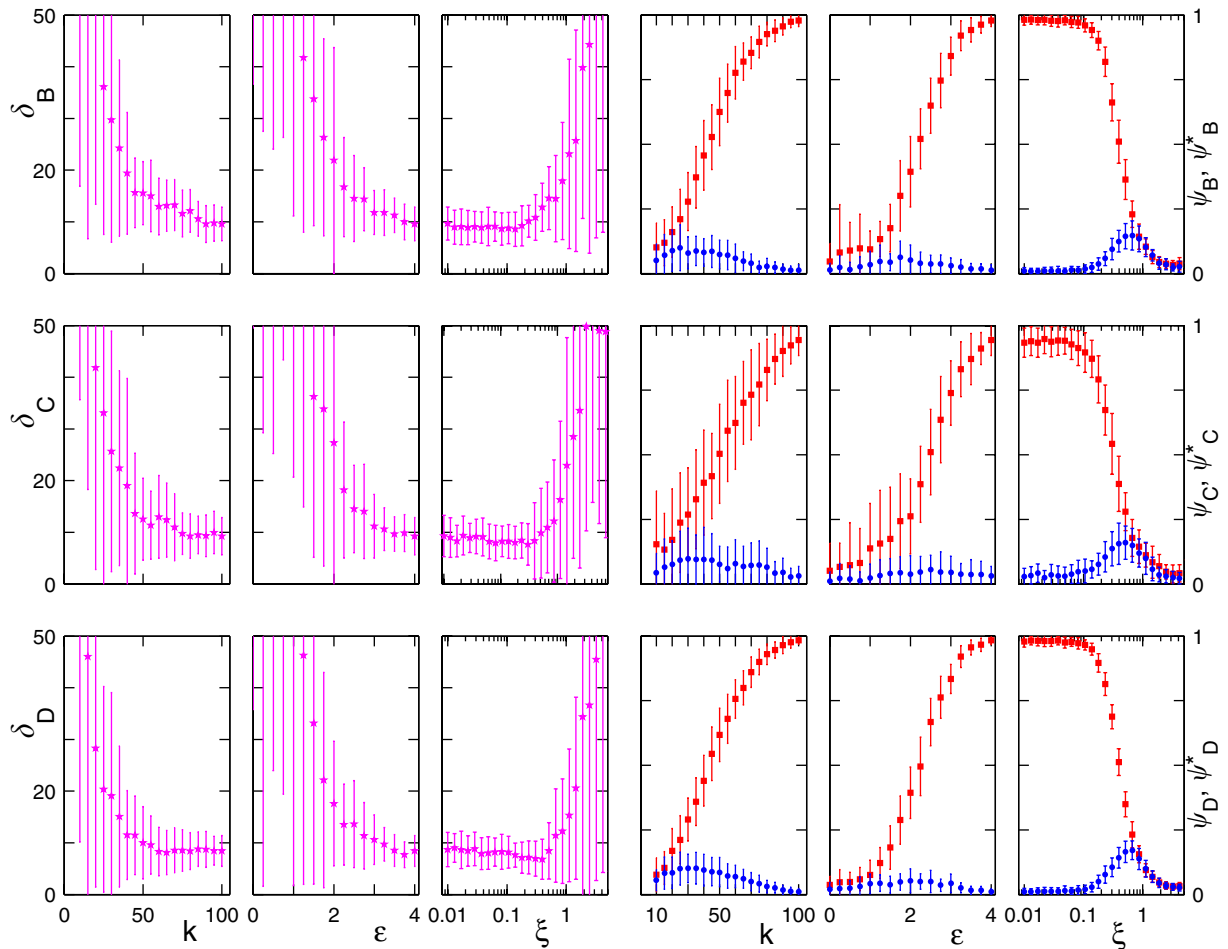


**Figure 2.** Dependence of  $\delta$  ( $\star$ ),  $\psi$  ( $\blacksquare$ ) and  $\psi^*$  ( $\bullet$ ) on the coupling strength  $\varepsilon$ , number of realizations  $k$ , and noise level  $\xi$  calculated for 50 independent sets of each  $k$  realizations. Symbols and error bars correspond to the mean  $\pm 1$  S.D. obtained for these 50 sets.

differences in  $\delta$  can be due to both this asymmetry and the different preceding states (uncoupled state for  $\mathcal{B}$  and the opposite coupling direction for  $\mathcal{C}$ ,  $\mathcal{D}$ ). For  $\psi$  also the length of the different intervals will be of influence. Therefore, we do not average  $\delta$  and  $\psi$  over  $\mathcal{B}$ ,  $\mathcal{C}$  and  $\mathcal{D}$  but rather consider individual values.

A decrease in the number of realizations  $k$  must lead to decreased discriminative power of  $H_i$ . Starting at  $\delta < 10$  for  $k = 100$ , a detection is still achieved within the first 20 samples down to  $k \approx 40$  for all three intervals (figure 2). Here and in the following we refer to the mean values of the performance measures. Furthermore, values of  $k \approx 50$  suffice to yield  $\psi > 0.5$ . Only for smaller  $k$  values, a reliable detection of the coupling direction becomes unfeasible. Distributions of  $\psi$  and  $\psi^*$  start overlapping, and  $\delta$  values rise strongly. We deliberately truncated the axis of  $\delta$  at 50. Broad distributions of  $\delta$  with higher mean values are compatible with scattered chance detections related to the nonzero size of the surrogate test and should not be further interpreted. The fact that only a few tens of realizations suffice to correctly track the time-dependent directional coupling

underlines the power of the proposed method. A view to the dependence on the coupling strength reveals that down to  $\varepsilon \approx 2.5$  a reliable detection of the coupling direction is possible. For very long time series from stationary dynamics certainly smaller couplings can be detected using statistics such as  $H$  (e.g. [13]). Nonetheless, the sensitivity of  $H_i$  for weak couplings appears very good. In analogy to conventional measures of directional coupling [1, 3], the information of directionality cannot be properly derived from  $H_i$  for very strong couplings resulting in synchronous motion. The entire coupling range investigated here corresponds to non-synchronous motion since the maximal conditional Lyapunov exponent becomes negative only at  $\varepsilon \approx 13$  and 10 for couplings from  $X$  to  $Y$  and  $Y$  to  $X$ , respectively.<sup>5</sup> Finally, we added uncorrelated Gaussian noise to both signals with amplitudes quantified by the ratio of the variances  $\xi = \sigma_{\text{noise}}^2 / \sigma_{\text{signal}}^2$ . Up to  $\xi \approx 0.3$ , we get  $\psi > 0.5$  and  $\delta < 20$ . Only for higher noise levels  $\psi$  and  $\psi^*$  start overlapping. The performance of  $H_i$  degrades smoothly with increasing noise levels. We emphasize that one oscillation of the dynamics corresponds to about 20 samples (figure 1(a)). Hence, for wide ranges of  $k$ ,  $\varepsilon$  and  $\xi$ , our approach allows detecting the directional couplings within the first oscillation after their onset. Such a high temporal resolution could certainly not be obtained by means of conventional moving window techniques.

Dealing with the same setting addressed here, [20] pooled all delay vectors  $\{\mathbf{x}_i^j, \mathbf{y}_i^j\}_{i=\eta, \dots, n}^{j=1, \dots, k}$  (cf [21, 22]) and proposed a specific constraint on the nearest neighbour search. However, in contrast to our approach, this technique is acausal. For any given time, information from the entire time series can enter the statistics. In particular, an interference of information from uncoupled and coupled periods can occur, potentially resulting in false positive and false negative detections of directional couplings.

In neuroscience, time-resolved averages across realizations are standard in the analysis of so-called event-related potentials [23]. In this context, phase synchronization measures based on temporal averages of phase differences have been adapted to estimate phase clustering across realizations [24]. While, in this respect, these techniques are similar to our approach, they do not allow determining coupling directions. To determine the direction of the coupling underlying phase clustering across realizations, an adaptation of the evolution map approach [1] should be considered. Directional information can be obtained from linear causality measures applied in a time-resolved manner across realizations [25]. However, linear measures are not in general sensitive to couplings between nonlinear dynamics.

The application to a Lorenz dynamics illustrated the power of our approach, and we are confident that  $H_i$  inherits the wide applicability to various dynamics from  $H$  (e.g. [12, 13]). Furthermore, the surrogate procedure applied here can also account for time-dependent offsets due to non-stationarities unrelated to time-dependent couplings. In conclusion, our technique can significantly advance the analysis of event-related time-dependent directional couplings. Furthermore, note that  $H_i$  itself is only an example of an application of embeddings across realizations. Any metric bi- or univariate measure such as mutual information or correlation dimension [15] can be adapted to serve as time-resolved causal statistics to characterize various aspects of time-dependent state space structures.<sup>6</sup> Hence, beyond the particular application proposed here, our approach is of general applicability.

<sup>5</sup> Note that we are aware of the discrepancy of the latter zero crossing with results reported in [19].

<sup>6</sup> Dynamical measures such as (mutual) prediction errors [15], which explicitly analyse the interrelation of subsequent samples, cannot be used.

## Acknowledgments

RGA was supported by a Feodor Lynen-fellowship of the Alexander von Humboldt-Foundation. AL was supported by the Juan de la Cierva Program. We are grateful to S Astakhov, P Grassberger, A S Pikovsky, M G Rosenblum and D A Smirnov for useful discussions.

## References

- [1] Rosenblum M G and Pikovsky A S 2001 *Phys. Rev. E* **64** 045202
- [2] Schiff S J, So P, Chang T, Burke R E and Sauer T 1996 *Phys. Rev. E* **54** 6708
- [3] Arnold J, Lehnertz K, Grassberger P and Elger C E 1999 *Physica D* **134** 419
- [4] Stam C J and van Dijk B W 2002 *Physica D* **163** 236
- [5] Bhattacharya J, Pereda E, Kariyappa R and Kanjilal P 2001 *Sol. Phys.* **199** 267
- [6] Rosenblum M G, Cimponeriu L, Bezerianos A, Patzak A and Mrowka R 2002 *Phys. Rev. E* **65** 041909
- [7] Stam C, Breakspear M, van Capellen van Walsum A-M and van Dijk B W 2003 *Human Brain Mapping* **19** 63
- [8] Breakspear M, Terry J R, Friston K, Harris A, Williams L, Brown K, Brennan J and Gordon E 2003 *Neuroimage* **20** 466
- [9] Todd M, Erickson K, Chang L, Lee K and Nichols J 2004 *Chaos* **14** 387
- [10] Mormann F, Kreuz T, Rieke C, Andrzejak R G, David P, Elger C E and Lehnertz K 2005 *Clin. Neurophysiol.* **116** 569
- [11] Takens F 1981 *Dynamical Systems and Turbulence (Lecture Notes in Mathematics vol 898)* ed D A Rand and L-S Young (Berlin: Springer)
- [12] Quiñero R, Arnhold A and Grassberger P 2000 *Phys. Rev. E* **61** 5142
- [13] Smirnov D A and Andrzejak R G 2005 *Phys. Rev. E* **71** 036207
- [14] Theiler J 1986 *Phys. Rev. A* **34** 2427
- [15] Kantz H and Schreiber T 1997 *Nonlinear Time Series Analysis* (Cambridge: Cambridge University Press)
- [16] Theiler J, Eubank S, Longtin A, Galdrikian B and Farmer J D 1992 *Physica D* **58** 77
- [17] Prichard D and Theiler J 1994 *Phys. Rev. Lett.* **73** 951
- [18] Lorenz E N 1963 *J. Atmos. Sci.* **20** 130
- [19] Zheng Z and Hu G 2000 *Phys. Rev. E* **62** 7882
- [20] Kramer M A, Edwards E, Soltani M, Berger M S, Knight R T and Szeri A J 2004 *Phys. Rev. E* **70** 011914
- [21] János I M and Tél T 1994 *Phys. Rev. E* **49** 2756
- [22] Efferen A, Lehnertz K, Schreiber T, Grunwald T, David P and Elger C E 2000 *Physica D* **140** 257
- [23] Dawson G D 1951 *J. Physiol.* **115** p 2
- [24] Fell J, Klaver P, Lehnertz K, Grunwald T, Schaller C, Elger C E and Fernández G 2001 *Nat. Neurosci.* **4** 1259
- [25] Kaminski M, Ding M, Truccolo W A and Bressler S L 2001 *Biol. Cybern* **85** 145